SELF-FOCUSING OF HERMITE-COSH-GAUSSIAN LASER BEAMS IN A PLASMA UNDER A WEAKLY RELATIVISTIC AND PONDEROMOTIVE REGIME

K. M. Gavade [1], T. U. Urunkar [1], B. D. Vhanmore [1], A. T. Valkunde [1], M. V. Takale [1*], S. D. Patil [2]

[1] Department of Physics, Shivaji University, Kolhapur 416 004, India; e-mail: mvtphyunishivaji@gmail.com
[2] Department of Physics, Devchand College, Arjunnagar, Kolhapur 591 237, India

In the theoretical investigation of the self-focusing of elegant Hermite-Cosh-Gaussian (EHChG) beams, the crucial role of decentred parameters has been explored thoroughly in the case of the weak relativistic and ponderomotive regime of interaction. In the present study, the cartesian coordinate system has been employed, which enables us to study the evolution of two transverse beam-width parameters simultaneously. The differential equations for the beam-width parameters are set up through the parabolic wave equation approach by following WKB and paraxial approximations.

Keywords: *self-focusing, elegant Hermite-Cosh-Gaussian laser beam, decentered parameter, relativistic, ponderomotive.*

САМОФОКУСИРОВКА ЛАЗЕРНЫХ ПУЧКОВ ЭРМИТА-КОШИ-ГАУССА В ПЛАЗМЕ В СЛАБОРЕЛЯТИВИСТСКОМ ПОНДЕРОМОТОРНОМ РЕЖИМЕ

K. M. Gavade [1], T. U. Urunkar [1], B. D. Vhanmore [1], A. T. Valkunde [1], M. V. Takale [1*], S. D. Patil [2]

УДК 533.9;537.525.1

[1] Университет Шиваджи, Колхапур, 416004, Индия;
e-mail: mvtphyunishivaji@gmail.com
[2] Девчандский колледж, Арджуннагар, Колхапур, 591237, Индия

(Поступила 16 июля 2018)

При теоретическом исследовании самофокусировки лазерных пучков Эрмита-Коши-Гаусса изучена решающая роль параметров децентровки в случае слабого релятивистского и пондеромоторного режима взаимодействия. Использована декартова система координат, которая позволяет одновременно изучать эволюцию двух параметров, описывающих поперечные размеры пучка. Дифференциальные уравнения для ширины пучка устанавливаются с помощью параболического волнового уравнения в параксиальном приближении.

Ключевые слова: *самофокусировка, лазерный пучок Эрмита-Коши-Гаусса, децентрированный параметр, релятивистский, пондеромоторный.*

Introduction. The self-focusing of laser beams in plasmas has been a subject of many important applications, mainly because it considerably influences other nonlinear phenomena. Generally, the theory of self-focusing is well established with the propagation characteristics of the beams, which are found to be closely related to the properties of the medium. The self-focusing and de-focusing of laser beams in nonlinear media was reviewed by Akhmanov et al. [1] and extended to plasmas by Sodha et al. [2]. In this phenomenon, the dielectric constant of the plasma has been modified by the high-power laser beams. However, the increase of the relativistic mass of the electron leads to the modification of the dielectric constant of the plasma, which gives rise to relativistic self-focusing [3]. Another nonlinearity caused by the transverse ponderomotive force, which is generated by the intensity gradient of the laser beam, pushes electrons from the central region of the beam and depresses the electron density. As a result, the dielectric constant of the plasma is modified, producing ponderomotive self-focusing [4]. It has been further established that the combined effects of relativistic and ponderomotive nonlinearities are also important [5–7]. Recently, the effect of light absorption and temperature on the self-focusing of finite Airy-Gaussian beams have been studied by Ouahid et al. [8] in a plasma with the relativistic and ponderomotive regime. The self-focusing of elliptic Gaussian laser beams in a relativistic ponderomotive plasma using a ramp density profile has been studied by Kumar et al. [9]. Patil et al. [10–12] studied the influence of light absorption on the self-focusing at the laser-plasma interaction with weak relativistic-ponderomotive nonlinearity.

On the other hand, most of the theoretical investigations on the self-focusing of laser beams in plasmas are, however, limited to the beams that exhibit the Gaussian intensity profile. However, in many situations of interest, there is a decentering of intensity distribution along the wavefront of the beam. Patil et al. [13, 14] analytically investigated the self-focusing of Hermite-Cosh-Gaussian laser beams in semiconductors. Recently, Valkunde et al. [15] studied the domain of the decentered parameter and its effect on the self-focusing of Hermite-Cosh-Gaussian laser beams in a collisional plasma. A new class of the laser beam, which is a more general case for an elegant Hermite-Gaussian beam and Cosh-Gaussian beam, i.e., elegant Hermite-Cosh-Gaussian (EHChG), was studied by Honarasa and Keshavarz [16] for its propagation properties. As such, the nonlinear effects caused by the propagation of such laser beams through plasmas are highly sensitive to the laser-plasma coupling parameters. Thus, such beams can be utilized to achieve efficient interaction with plasmas. Recently, Vhanmore et al. [17, 18] explored the effect of the decentered parameter on the self-focusing of asymmetric Cosh-Gaussian laser beams propagating through a collisionless magnetized plasma.

This paper presents an analysis of the self-focusing of elegant Hermite-Cosh-Gaussian (EHChG) beams in a plasma under a weakly relativistic and ponderomotive regime. The differential equations for the beam-width parameters are established through the usual parabolic wave equation approach by following WKB and paraxial approximations. The variation of the beam width parameters with the dimensionless distance of propagation is shown graphically for different values of two identical transverse decentered parameters. Eventually, the comparison of the beam width parameter variation between two modes reveals interesting dynamics related to the intensity profiles of individual modes and in turn the use of the identical decentered parameters deployed.

Evolution of beam-width parameters. The electric field distribution of EHChG laser beams at the plane of $z = 0$ is described as [16]:

$$E(x,y,z) = E_0 H_0\left(\frac{x}{r_0}\right) H_p\left(\frac{y}{r_0}\right)\cosh(\Omega_1 x)\cosh(\Omega_2 y)\exp\left[-\left(\frac{x^2+y^2}{r_0^2}\right)\right], \quad (1)$$

where, H_0 and H_p are 0^{th} order and p^{th} order Hermite polynomials, E_0 and r_0 are the initial amplitude of the electric field and initial beam radius, $\Omega_1 = b_1/r_0$ and $\Omega_2 = b_2/r_0$ are the parameters associated with the hyperbolic cosine functions, called also the cosh factors, with b_1 and b_2 the respective decentered parameters in x and y dimensions. Such decentered laser beams can be produced in the laboratory by offsetting a collimating lens away from the beam axis for achieving intensity distribution in the wide area and versatility in a spot shape [19]. Figure 1a depicts the density plot of the initial intensity distribution for the TEM_{00} mode with different identical decentered parameters in the transverse dimensions of EHChG beams. From this figure, it is clear that for identical decentered parameters, the TEM_{00} mode of the laser recovers its circularly symmetric (Gaussian) distribution of intensity. With increase in the decentered parameter, the intensity is distributed in the wide area. Figure 1b portrays the corresponding initial intensity distribution for the TEM_{02} mode. It shows a slight deviation from the circular symmetry. As expected, such deviation is more in the y dimension than the x dimension of the beam. It is to be noted that with identical decentering of the beam profile, the TEM_{02} mode gives the elliptic initial intensity distribution rather than the TEM_{00} mode. Such elliptic nature of the initial intensity distribution will further explain the essence of the non-monotonic dependence of the initial beam radii in transverse dimensions during propagation.

The propagation of laser beams through plasmas is characterized by the dielectric function which can, in general, be expressed as [2]:

$$\varepsilon = \varepsilon_0 + \phi(EE^*). \quad (2)$$

Here $\varepsilon = 1-(\omega_p^2/\omega^2)$ and ϕ are the linear and nonlinear part of the dielectric function, $\omega_p = (4\pi n_0 e^2/m_0)^{1/2}$ is the plasma frequency, e and m_0 are the charge and rest mass of the electron, n_0 is the density of plasma electrons in the absence of the beam, and ω is the angular frequency of the laser used.

In the weakly relativistic and ponderomotive regime, the nonlinear dielectric function has the following form [20, 21]

$$\phi(EE^*) = \frac{\omega_p^2}{\omega^2}\left[1 - \frac{1}{\gamma}\exp\left[-\beta(\gamma - 1)\right]\right], \tag{3}$$

where $\gamma = (1 + \alpha EE^*)^{1/2}$, $\alpha = e^2/m^2\omega^2c^2$, $\beta = m_0c^2/T_0$, ω is the angular frequency of the laser used, and T_0 is the equilibrium plasma electron temperature.

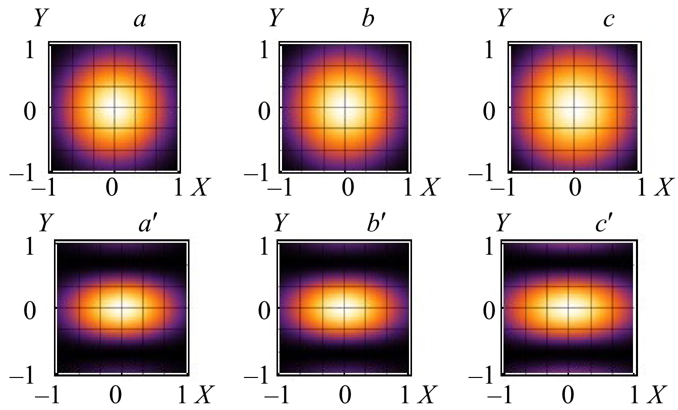

Fig. 1. Density plot of the initial intensity distribution of EHChG beams for the TEM_{00} (*a*–*c*) and TEM_{02} modes (*a*′–*c*′); $b_1 = b_2 = 0.0$ (*a*, *a*′), 0.4 (*b*, *b*′), 0.8 (*c*, *c*′).

The wave equation governing the electric field E of the beam in a plasma with the dielectric function can be written as

$$\nabla^2 E + (\omega^2 / c^2)\varepsilon E + \nabla\left(E(\nabla\varepsilon / \varepsilon)\right) = 0\,. \tag{4}$$

The last term on the left-hand side of Eq. (4) can be neglected provided that $k^{-2}\nabla^2(\ln\varepsilon) \sim 1$, where, $k = (\omega / c)\sqrt{\varepsilon_0}$ is the wave number of the laser beam. Hence,

$$\nabla^2 E + (\omega^2 / c^2)\varepsilon E = 0\,. \tag{5}$$

We can express electric field of the laser beam as

$$E = A(x, y, z)\exp\left[i(\omega t - kz)\right], \tag{6}$$

where $A(x, y, z)$ is the complex amplitude of the electric field described by the parabolic equation in the WKB approximation:

$$2ik\frac{\partial A}{\partial z} = \frac{\partial^2 A}{\partial x^2} + \frac{\partial^2 A}{\partial y^2} + \frac{k^2}{\varepsilon_0}\phi\left(EE^*\right)A\,. \tag{7}$$

For solving Eq. (7), $A(x, y, z)$ can be expressed as

$$A(x, y, z) = A_{0p}(x, y, z)\exp\left[-ikS(x, y, z)\right], \tag{8}$$

where, A_{0p} and S are real functions of x, y, and z. By inserting the expression of $A(x, y, z)$ from Eq. (8) into Eq. (7) and equating the real and imaginary parts, one obtains

$$2\frac{\partial S}{\partial z} + \left(\frac{\partial S}{\partial x}\right)^2 + \left(\frac{\partial S}{\partial y}\right)^2 = \frac{1}{k^2 A_{0p}}\left(\frac{\partial^2 A_{0p}}{\partial x^2} + \frac{\partial^2 A_{0p}}{\partial y^2}\right) + \frac{\phi\left(A_{0p}\right)}{\varepsilon_0}, \tag{9}$$

$$\frac{\partial A_{0p}^2}{\partial z} + \frac{\partial S}{\partial x}\frac{\partial A_{0p}^2}{\partial x} + \frac{\partial S}{\partial y}\frac{\partial A_{0p}^2}{\partial y} + \left(\frac{\partial^2 S}{\partial x^2} + \frac{\partial^2 S}{\partial y^2}\right)A_{0p}^2 = 0\,. \tag{10}$$

Following the approach given by Akhmanov et al. [1] and its extension by Sodha et al. [2], the solutions corresponding to Eqs. (9) and (10) are given by

$$S = \frac{x^2}{2f_1}\frac{df_1}{dz} + \frac{y^2}{2f_2}\frac{df_2}{dz} + \varphi(z), \tag{11}$$

$$A_{0p}^2=\frac{E_0^2}{f_1f_2}\left[H_0\left(\frac{x}{r_0f_1}\right)H_p\left(\frac{y}{r_0f_2}\right)\right]^2\left[\cosh\left(\frac{b_1x}{r_0f_1}\right)\cosh\left(\frac{b_2y}{r_0f_2}\right)\right]^2\exp\left[-2\left(\frac{x^2}{r_0^2f_1^2}+\frac{y^2}{r_0^2f_2^2}\right)\right]. \quad (12)$$

Finally, after some algebraic manipulations, the nonlinear coupled differential equations for dimensionless beam-width parameters f_1 and f_2 are expressed as follows:

For the TEM_{00} mode:

$$\frac{d^2f_1}{d\eta^2}=\frac{A_1}{f_1^3}-\frac{\rho_1^2B_1P\omega_p^2\exp\left\{\beta-\beta\sqrt{1+\frac{P}{f_1f_2}}\right\}\left\{P\beta+\left(\beta+\sqrt{1+\frac{P}{f_1f_2}}\right)f_2\right\}}{2\omega^2f_1^2f_2\left(P+f_1f_2\right)^2}, \quad (13)$$

$$\frac{d^2f_2}{d\eta^2}=\frac{A_2}{f_2^3}-\frac{\rho_2^2B_2P\omega_p^2\exp\left\{\beta-\beta\sqrt{1+\frac{P}{f_1f_2}}\right\}\left\{P\beta+\left(\beta+\sqrt{1+\frac{P}{f_1f_2}}\right)f_1\right\}}{2\omega^2f_2^2f_1\left(P+f_1f_2\right)^2}.$$

For the TEM_{02} mode:

$$\frac{d^2f_1}{d\eta^2}=\frac{A_1}{f_1^3}-\frac{8\rho_1^2B_1P\omega_p^2\exp\left\{\beta-\beta\sqrt{1+\frac{4P}{f_1f_2}}\right\}\left\{4P\beta+\left(\beta+\sqrt{1+\frac{4P}{f_1f_2}}\right)f_2\right\}}{\omega^2f_1^2f_2\left(4P+f_1f_2\right)^2}, \quad (14)$$

$$\frac{d^2f_2}{d\eta^2}=\frac{3A_2}{f_2^3}-\frac{8\rho_2^2\left(4-B_2\right)P\omega_p^2\exp\left\{\beta-\beta\sqrt{1+\frac{4P}{f_1f_2}}\right\}\left\{4P\beta+\left(\beta+\sqrt{1+\frac{4P}{f_1f_2}}\right)f_1\right\}}{2\omega^2f_2^2f_1\left(4P+f_1f_2\right)^2},$$

where, $A_{1,2}=4(1-b_{1,2}^2)$, $B_{1,2}=(2-b_{1,2}^2)$, $P=\alpha E_0^2$, $\rho_1=\rho_2=r_0\omega/c$ is the equilibrium beam radius, and $\eta = z/kr_0^2$ is the dimensionless distance of propagation. Under the critical condition, $f_1=f_2=1$ at $\eta=0$, the condition $d^2f_1/d\eta^2=d^2f_2/d\eta^2=0$ leads to the propagation of EHChG laser beams without convergence or divergence, i.e., the laser beam propagates in the self-trapped mode. By using this condition in Eqs. (13) and (14), one can obtain relations between ρ_1 and ρ_2 as:

For the TEM_{00} mode $\rho_1=\rho_2=\rho$:

$$\rho^2=\frac{2A_1\left(1+P\right)^2\omega^2}{B_1P\omega_p^2\exp\left\{\beta-\beta\sqrt{1+P}\right\}\left\{P\beta+\left(\beta+\sqrt{1+P}\right)\right\}}. \quad (15)$$

For the TEM_{02} mode $\rho_1\neq\rho_2$:

$$\rho_1^2=\frac{A_1\left(1+4P\right)^2\omega^2}{8B_1P\omega_p^2\exp\left\{\beta-\beta\sqrt{1+4P}\right\}\left\{4P\beta+\left(\beta+\sqrt{1+4P}\right)\right\}}, \quad (16)$$

$$\rho_2^2=\frac{3A_2\left(1+4P\right)^2\omega^2}{8\left(4-B_2\right)P\omega_p^2\exp\left\{\beta-\beta\sqrt{1+4P}\right\}\left\{4P\beta+\left(\beta+\sqrt{1+4P}\right)\right\}}. \quad (17)$$

Results and discussion. Equations (13) and (14) are definitely more amenable to mathematical manipulations. These equations are second-order, nonlinear, coupled, differential equations. On the right-hand side of these equations, the first term corresponds to the diffraction divergence of the beam, and the second term corresponds to nonlinear refraction, responsible for the self-focusing of the beam. We have solved these equations numerically by using the fourth-order Runge-Kutta method for the numerical values of the laser-plasma parameters, $\omega = 1.778\times10^{14}$ rad/s, $\beta = 5$, $n_0 = 10^{19}$ cm^{-3}, and $b_1 = b_2 = 0.0, 0.4, 0.8$. If the dimensionless initial beam radii ρ_1 and ρ_2, and dimensionless intensity parameter P satisfy Eqs. (15) and (16), we will have $d^2f_{1,2}/d\eta^2 = 0$ at $\eta = 0$, ensuring that $df_{1,2}/d\eta$ and $f_{1,2}$ retain their initial boundary values throughout the path of propagation; such propagation without the change in beam width is called uniform waveguide propagation. The dependence of ρ versus P according to Eqs. (15) and (16) is known as the self-trapped condition or the critical curve. The parameter $d^2f_{1,2}/d\eta^2$ vanishes if the point (P, $f_1=f_2=1$) falls on the critical curve. The parameter $d^2f_{1,2}/d\eta^2$ has a positive value if the point (P, ρ) falls below the critical curve, and it has a negative value if the point lies above the curve, which corresponds to the self-defocused and self-focused region, respectively.

For the TEM_{00} mode, Fig. 2a shows the plot of the initial beam radii ρ_1 and ρ_2 against the initial intensity parameter P under the variation of identical decentered parameters $b_1 = b_2 = 0.0$, 0.4, 0.8. From Fig. 2a, it is seen that as the value of the decentered parameter increases, the critical curves shift downward. One should note that the initial beam radii ρ_1 and ρ_2 corresponding to two transverse dimensions vary synchronously with P, which is also evident from the symmetry observed in Eq. (15), i.e., $\rho_1 = \rho_2 = \rho$. A simple inspection of Eq. (15) clearly reveals that it can be arranged as quadratic in variable P. Therefore, there are two possible values of P that correspond to the unique initial beam radius. Such a unique value of ρ decreases with increase in the associated decentered parameter values.

Figure 2b shows the variation of ρ_1 and ρ_2 with P for the TEM_{02} mode of the laser under the same identical values of b_1 and b_2 as those in Fig. 2a. From Fig. 2b, it is observed that as the value of the decentered parameter increases, the nature of the critical curves is the same as that discussed in Fig. 2a for the TEM_{00} mode. However, ρ_1 and ρ_2 do not vary synchronously with P. Due to this there are two different initial beam radii corresponding to two possible values of P, which is also apparent from the difference in Eqs. (16) and (17). It is also evident from Fig. 2b that the minimum value of ρ_2 is always less than ρ_1 for every curve.

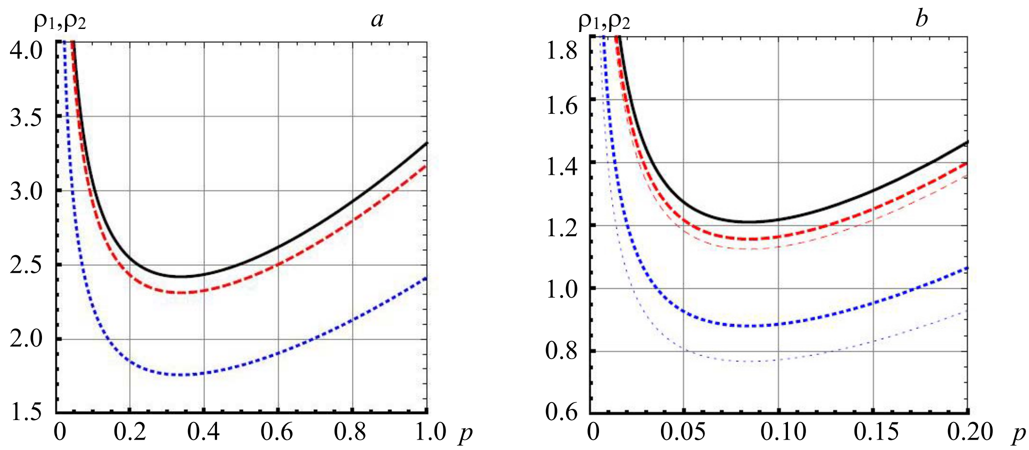

Fig. 2. Dependence of the dimensionless initial beam radii as a function of the intensity parameter P for the TEM_{00} (a) and TEM_{02} modes (b); $b_1 = b_2 = 0.0$ (solid curves), 0.4 (dashed curves), and 0.8 (dotted curves). Thick curves are for ρ_1 and thin curves are for ρ_2.

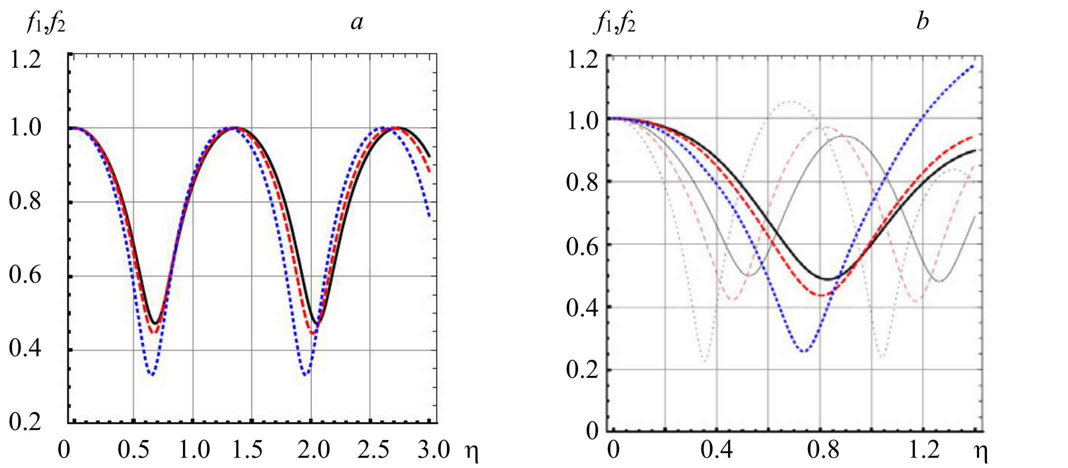

Fig. 3. Variation of the beam-width parameters as a function of the dimensionless distance of propagation for the TEM_{00} (a) and TEM_{02} modes (b); $b_1 = b_2 = 0.0$ (solid curves), 0.4 (dashed curves), and 0.8 (dotted curves). Thick curves are for f_1 and thin curves are for f_2.

Such non-monotonic change of ρ_1 and ρ_2 in the transverse dimensions of the beam is due to the extent of the Hermite polynomial in the y dimension of the beam, which gives the elliptic nature of the initial intensity distribution of the TEM_{02} mode.

Figure 3a depicts the variation of two transverse beam-width parameters f_1 and f_2 against the dimensionless distance of propagation η for the TEM_{00} mode. The initial conditions were set as $\rho = 2.8$ and $P = 0.4$, and we varied the values of the decentered parameters in the transverse dimensions of the beam, $b_1 = b_2 = 0.0, 0.4, 0.8$. One should note that both beam-width parameters show a synchronized oscillatory character during propagation. This is due to the symmetric nature of the TEM_{00} mode of the laser. As the value of the decentered parameter increases, enhanced self-focusing is observed, with the subsequent reduction in the self-focusing length in both dimensions of the beam.

Figure 3b shows the variation of f_1 and f_2 against η for the TEM_{02} mode of the laser at $\rho = 1.4$ and $P = 0.1$. One should note that as the values of the decentered parameter increases, complexity in the beam-width parameters is observed. This is due to the asymmetry in the intensity distribution of the TEM_{02} mode of the beam. The complexity in f_2 is more than that in f_1. As obviously, with increase in the decentered parameter in both dimensions of the beam, enhanced self-focusing is observed.

Conclusions. The nonlinear coupled differential equations for the transverse beam-width parameters of EHChG beam propagation in a plasma are established under a weakly relativistic and ponderomotive regime. Intricacy in self-focusing phenomenon is observed as one considers the higher-order mode index. The following important conclusions are drawn from the present analysis.

With increase in the decentered parameter in both dimensions of the beam, there is an increase in the extent of self-focusing, with the subsequent reduction in the self-focusing length. With identical decentering of the beam profile in both the dimensions, a synchronized oscillatory character of the beam-width parameters is possible for the TEM_{00} mode, while they do not vary synchronously for the TEM_{02} mode of the laser. Complexity in the beam-width parameters of the beam increases with increase in the mode index of the beam profile. It would be interesting to study such a beam in various situations of laser-plasma interaction so as to explore the dynamics of the laser beam in two transverse dimensions simultaneously.

REFERENCES

1. S. A. Akhmanov, A. P. Sukhorukov, R. V. Khokhlov, *Sov. Phys. Usp.*, **10**, 609–636 (1968).
2. M. S. Sodha, A. K. Ghatak, V. K. Tripathi, *Prog. Opt.,* **13**, 169–265 (1976).
3. H. S. Brandi, C. Manus, G. Mainfray, *Phys. Rev. E*, **47**, 3780–3783 (1993).
4. F. Osman, R. Castillo, H. Hora, *J. Plasma Phys.,* **61**, 263–273 (1999).
5. S. D. Patil, M. V. Takale, V. J. Fulari, D. N. Gupta, H. Suk, *Appl. Phys. B*, **111**, 1–6 (2013).
6. S. D. Patil, M. V. Takale, *Phys. Plasmas*, **20**, 083101 (2013).
7. S. D. Patil, M. V. Takale, *Laser Phys. Lett.*, **10**, 115402 (2013).
8. L. Ouahid, L. Dalil-Essakali, A. Belafhal, *Opt. Quant. Electron.,* **50**, 216 (2018).
9. H. Kumar, M. Aggarwal, T. S. Gill, *J. Opt. Soc. Am. B*, **35**, 1635 (2018).
10. S. D. Patil, M. V. Takale, *AIP Conf. Proc.*, **1728**, 020129 (2016).
11. S. D. Patil, M. V. Takale, V. J. Fulari, T. S. Gill, *Laser Part. Beams*, **34**, 669–674 (2016).
12. S. D. Patil, P. P. Chikode, M.V. Takale, *J. Opt.,* **47**, 174–179 (2018).
13. S. D. Patil, M. V. Takale, M. B. Dongare, *Opt. Commun.,* **281**, 4776–4779 (2008).
14. S. Patil, M. Takale, V. Fulari, M. Dongare, *J. Mod. Opt.,* **55**, 3529–3535 (2008).
15. A. T. Valkunde, S. D. Patil, B. D. Vhanmore, T. U. Urunkar, K. M. Gavade, M. V. Takale, V. J. Fulari, *Phys. Plasmas*, **25**, 033103 (2018).
16. G. Honarasa, A. Keshavarz, *Optik*, **124**, 6535–6538 (2013).
17. B. D. Vhanmore, S. D. Patil, A. T. Valkunde, T. U. Urunkar, K. M. Gavade, M. V. Takale, *Laser Part. Beams*, **35**, 670–676 (2017).
18. B. D. Vhanmore, A. T. Valkunde, T. U. Urunkar, K. M. Gavade, S. D. Patil, M. V. Takale, *AIP Conf. Proc.*, **1953**, 140047 (2018).
19. M. Zhang, H. He, J. Dong, *IEEE Photon. J.*, **9**, 1501214 (2017).
20. T. S. Gill, R. Mahajan, R. Kaur, *Phys. Plasmas*, **18**, 033110 (2011).
21. M. R. J. Milani, A. R. Niknam, B. Bokaei, *IEEE Trans. Plasma Sci.*, **42**, 742–747 (2014).